
Supplementary information

Thymic epithelial cells amplify epigenetic noise to promote immune tolerance

In the format provided by the
authors and unedited

SUPPLEMENTARY INFORMATION

Thymic epithelial cells amplify epigenetic noise to promote immune tolerance

Noah Gamble^{1,2}, Jason A. Caldwell¹, Joshua McKeever^{1,3}, Caroline Kaiser^{1,4}, Alexandra Bradu¹, Peyton J. Dooley¹, Sandy Klemm⁵, William J. Greenleaf^{5,6,7,8}, Narutoshi Hibino^{9,10}, Aaron R. Dinner^{11,12,13} and Andrew S. Koh^{1,13,*}

¹Department of Pathology, University of Chicago; Chicago, IL, USA.

²Graduate Program in Biophysical Sciences, University of Chicago; Chicago, IL, USA.

³Committee on Molecular Metabolism and Nutrition, University of Chicago; Chicago, IL, USA.

⁴Department of Human Genetics, University of Chicago; Chicago, IL, USA.

⁵Department of Genetics, Stanford University; Stanford, CA, USA.

⁶Department of Applied Physics, Stanford University; Stanford, CA, USA.

⁷Department of Computer Science, Stanford University; Stanford, CA, USA.

⁸Chan Zuckerberg Biohub; San Francisco, CA, USA.

⁹Department of Surgery, University of Chicago; Chicago, IL, USA.

¹⁰Department of Cardiovascular Surgery, Advocate Children's Hospital; Chicago, IL, USA.

¹¹Department of Chemistry, University of Chicago; Chicago, IL, USA.

¹²James Franck Institute, University of Chicago; Chicago, IL, USA.

¹³Institute for Biophysical Dynamics, University of Chicago; Chicago, IL, USA.

*Correspondence: akoh@uchicago.edu

Table of Contents

Supplementary Notes.....	2
Supplementary Figures.....	6
Supplementary Discussion.....	11
Supplementary References.....	13

Supplementary Notes

Human mTECs repress p53 and amplify chromatin noise

To determine whether the destabilization of nucleosome-dense regions and repression of p53 activity are conserved in human mTEC maturation, we jointly profiled the transcriptome and chromatin accessibility landscapes of individual FACS-sorted mTECs from a three-month-old donor using the 10X Multiome platform. Consistent with our previous observations, we found a marked decrease in the proportion of scATAC-seq fragments within peaks across the putative developmental trajectory and a reciprocal gain in out-of-peak fragments within broad ~100 kb regions flanking active tissue-specific genes (Supplementary Fig. 2a–h). These out-of-peak fragments were enriched for long nucleosomal fragments compared to scATAC-seq fragments within peaks, which together with the above results suggest that nucleosome-dense chromatin regions near tissue-specific genes become destabilized during human mTEC maturation (Supplementary Fig. 2i).

We also detected repression of p53 activity in mature *AIRE*-expressing mTECs compared to immature progenitors as indicated by: (i) the depletion of p53-binding motifs within the accessible genome (Supplementary Fig. 2j); (ii) the loss in transcription factor footprints and flanking accessibility at sites containing p53 binding motifs (Supplementary Fig. 2k); (iii) the loss in expression of p53 target genes (Supplementary Fig. 2l); (iv) the gain in expression of genes encoding negative regulators of p53 activity (Supplementary Fig. 2m–p); and (v) the loss in expression of genes encoding positive regulators of p53 activity (Supplementary Fig. 2m,q–t). In addition to the negative regulators *MDM2* and *SIRT1* being induced during human mTEC maturation, we found the genes encoding LSD1 (which demethylates p53 to inhibit its cooperative activity with the DNA repair factor 53BP1¹) and TRIM24 (which inhibits p53's capacity to overcome nucleosomal barriers²) upregulated in mature mTECs compared to immature progenitors (Supplementary Fig. 2m,p). Related to the increased levels of *SIRT1*, we also found the reciprocal downregulation of the gene encoding DBC-1 (*BRINP1*) which suppresses SIRT1-mediated deacetylation of p53^{3,4} to stabilize p53 (Supplementary Fig. 2m,s). By contrast, *TP53* levels did not change between immature and *AIRE*⁺ mTECs with only a brief

transcriptional induction detected in transit-amplifying mTECs that was quickly extinguished upon further maturation (Supplementary Fig. 2m,u). Taken together, these results indicate that the destabilization of nucleosome-dense regions and repression of p53 activity are conserved features of human mTEC maturation.

Effect of p53-hyperactivity versus p53-deficiency on mTEC plasticity

A previous study reported deleterious effects of p53-deficiency on mTEC differentiation and ectopic expression of tissue-specific genes, due to inhibition of the cell's responsiveness to NF- κ B signaling⁵, the primary determinant of mTEC development⁶⁻¹⁰. Indeed, we observed from our Multiome analyses robust expression of canonical p53 target genes, transcription factor footprinting at p53 target motifs and selective enrichment of p53 target motifs in the accessible genome of immature mTECs indicating robust p53 activity in these progenitors (Fig. 2h–k and Extended Data Fig. 3a–c).

To directly compare the impact of compromised mTEC differentiation in p53-deficient mice to the suppression of chromatin accessibility noise in p53-cHyper mice on ectopic expression of tissue-specific genes, we conducted bulk RNA-seq on FACS-sorted mature and immature mTECs from sex-matched *Trp53^{ff}; Foxn1^{Cre}* (p53-cKO) and *Trp53^{ff}* (p53-WT) littermates. We performed differential expression analysis in parallel with the bulk RNA-seq datasets used for the p53-cHyper vs. p53-WT comparison and found p53 deficiency to significantly inhibit the expression of 353 AIRE-dependent tissue-specific genes (α TSGs) compared to WT controls (Supplementary Fig. 3a). At the same statistical thresholds, we observed 1,212 α TSGs to be inhibited by p53-hyperactivity in p53-cHyper mTECs compared to p53-WT counterparts (Supplementary Fig. 3b). These results suggest that the effect of chromatin stabilization in p53-cHyper mTECs is >3.4-fold more deleterious than the effect of dysregulated mTEC maturation in p53-cKO mTECs on AIRE-dependent ectopic gene expression.

Chromatin noise elevates baseline enhancer activity

To determine whether the increased loading of Pol II near AIRE-dependent tissue-specific genes (α TSGs) reflects transcriptional initiation at known *cis*-regulatory elements, we mined annotated distal enhancers¹¹ from the ENCODE consortium and identified 99,840 characterized enhancers (~one quarter of total) from 23 tissues within +/-100 kb regions flanking α TSGs, 70,871 (71.0%) of which did not overlap with scATAC-seq peaks. We traced the out-of-peak Pol II ChIP-seq reads across these enhancers and found elevated levels of Pol II occupancy compared to those found at out-of-peak enhancers near the Silent loci (Supplementary Fig. 4a). This differential Pol II localization at out-of-peak enhancers near α TSGs was largely independent of AIRE-induced transcription with the aggregate occupancy within +/-500 bp of the enhancer centers being ~37.3% of that observed at enhancers near highly active housekeeping genes (Supplementary Fig. 4b,c). However, the magnitude of the differential Pol II occupancy at these enhancers was substantially lower than the total differential occupancy spanning the regions flanking α TSGs, potentially indicative of elevated Pol II loading at unannotated *cis*-regulatory elements across these loci (Fig. 4n and Supplementary Fig. 4a).

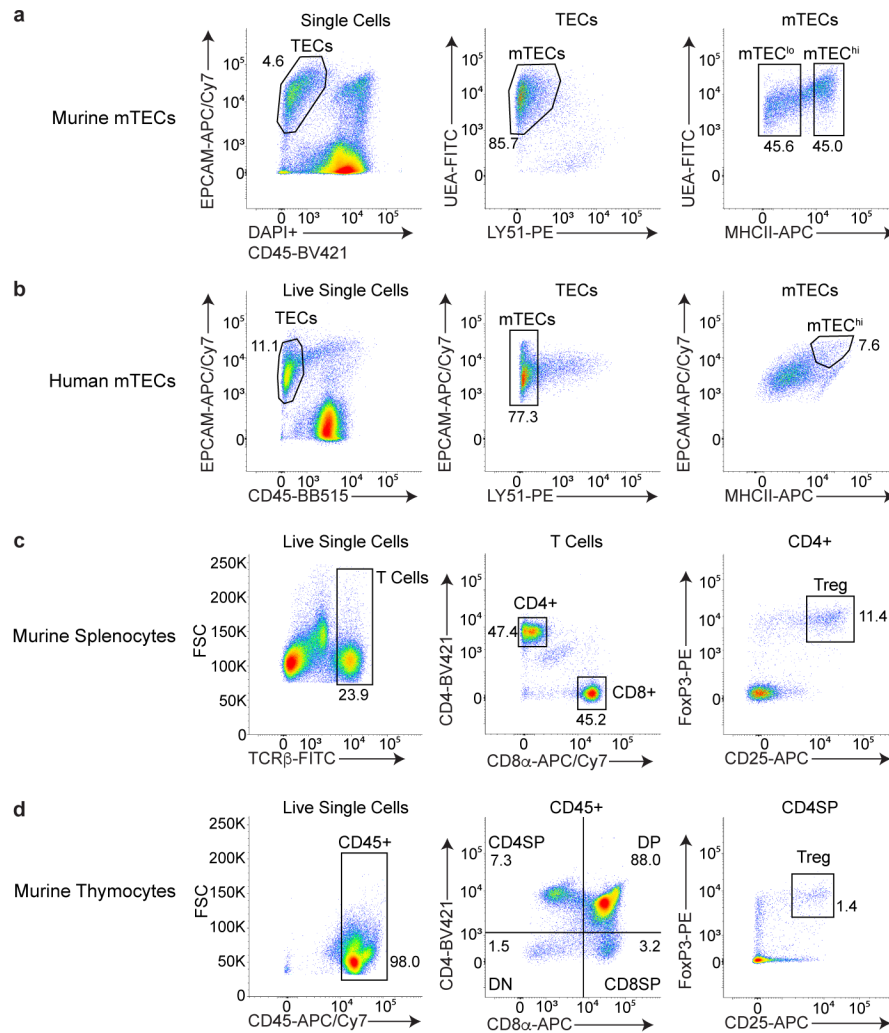
To determine whether heightened chromatin accessibility noise is associated with the elevated loading of Pol II at out-of-peak enhancers near α TSGs, we traced out-of-peak scATAC-seq fragments across these enhancers and detected focal signal at nearly all of them (98.5%), which in aggregate amounted to ~half (49.8%) of the accessibility amplitude observed at enhancers within peaks (Supplementary Fig. 4d,e). The magnitude of this chromatin destabilization at enhancers near α TSGs was significantly higher than that observed at enhancers near the Silent loci (Supplementary Fig. 4d–g). 34,495 out-of-peak enhancers near α TSGs (48.7% of total) exhibited accessibility at $\geq 1\%$ of maximum signal, and these regions exhibited aggregate accessibility greater than 2.5-fold of that observed at the 12,378 out-of-peak enhancers near the Silent loci (34.5% of total) that met the same 1% threshold (Supplementary Fig. 4d,g).

To determine whether the elevated Pol II loading at out-of-peak enhancers near α TSGs coincided with DNA damage, we profiled γ H2AX deposition and topoisomerase recruitment at these elements in *Aire*^{+/+} and *Aire*^{-/-} mTECs to find elevated levels of

γ H2AX, TOP2 α and TOP1 compared to those at out-of-peak enhancers near Silent loci that was largely AIRE-independent (Supplementary Fig. 4h–m). The magnitude of the DNA damage as measured by aggregate γ H2AX deposition within \pm 500 bp of the enhancer was \sim 40.1% of that observed at enhancers near highly active housekeeping genes (Supplementary Fig. 4n–p). Taken together, these results suggest a concordance between amplified chromatin accessibility noise, increased spurious transcriptional initiation at flanking enhancers, recruitment of topoisomerases, increased DNA damage, and p53-mediated triggering of cell death in p53-cHyper mTECs versus cellular plasticity in WT mTECs.

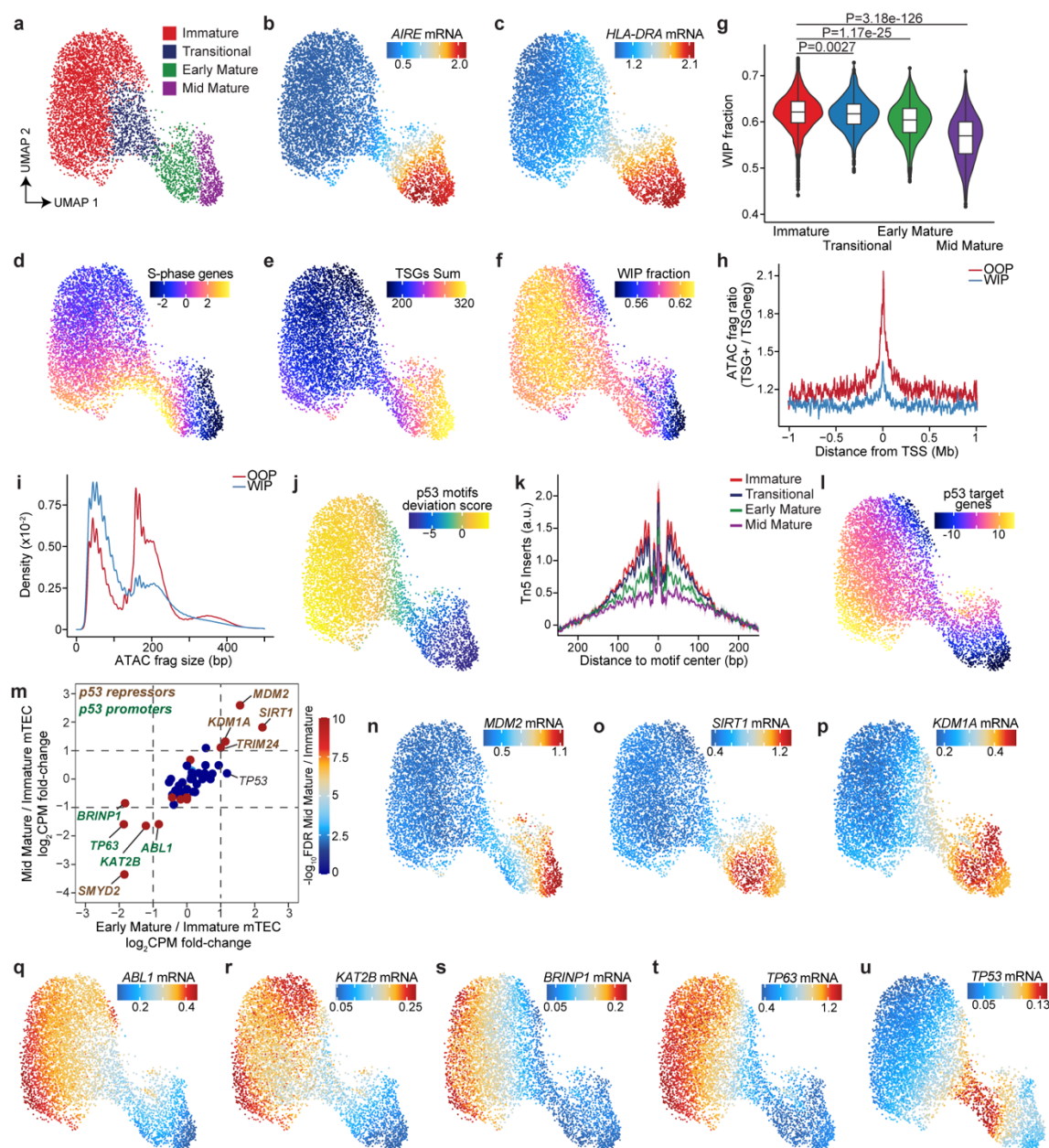
To quantify the potential contribution of the enhancer sequence content to the chromatin accessibility noise observed at out-of-peak enhancers near α TSGs, we performed *de novo* motif enrichment and found no correlation between enhancer AT-content and motif enrichment as the same AP-1 motifs represented the top 4 enriched motifs at out-of-peak enhancers near α TSG and Silent loci (Supplementary Fig. 4q,r). These results suggest that the chromatin destabilization over poly-AT tracts enriched at regions flanking α TSGs amplified the fluctuations in background chromatin accessibility at nearby enhancers, consistent with the influence of poly-A tracts on the nucleosome stability of neighboring flanking regions¹².

Supplementary Figures



Supplementary Fig. 1: Flow cytometry plots

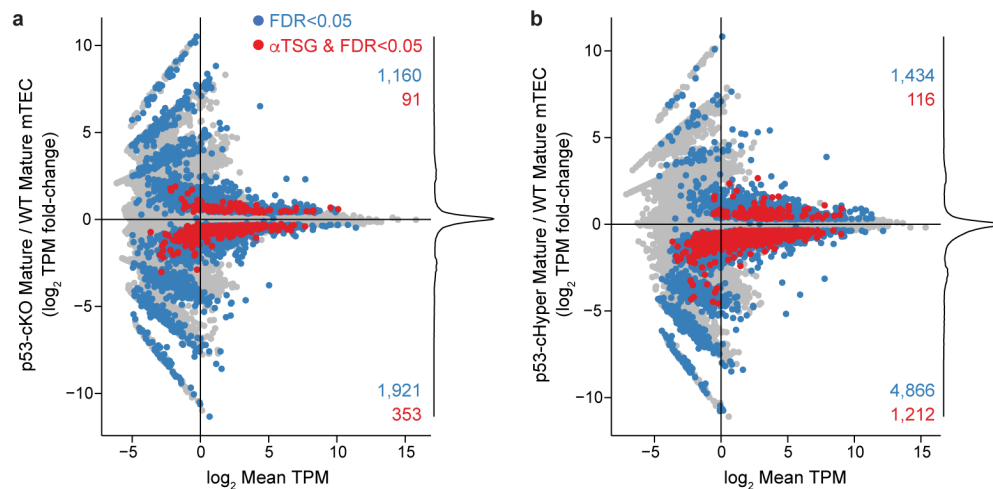
a–d, Representative flow cytometry plots for gating of indicated populations.



Supplementary Fig. 2: Human mTECs amplify chromatin accessibility noise and repress p53.

a, scATAC-seq UMAP of human mTECs, colored by cluster annotation. **b-d**, Gene expression levels of *AIRE* (**b**) or *HLA-DRA* (**c**) or module of S-phase genes (**d**) overlaid on scATAC-seq UMAP from (**a**). **e**, Sum of mRNA from all tissue-specific genes (TSGs) overlaid on scATAC-seq UMAP from (**a**). **f**, Fraction of scATAC-seq fragments within scATAC-seq peaks (WIP) overlaid on scATAC-seq UMAP defined in (**a**). **g**, Violin plots depicting the distributions of WIP fraction across annotated clusters of human mTECs (n

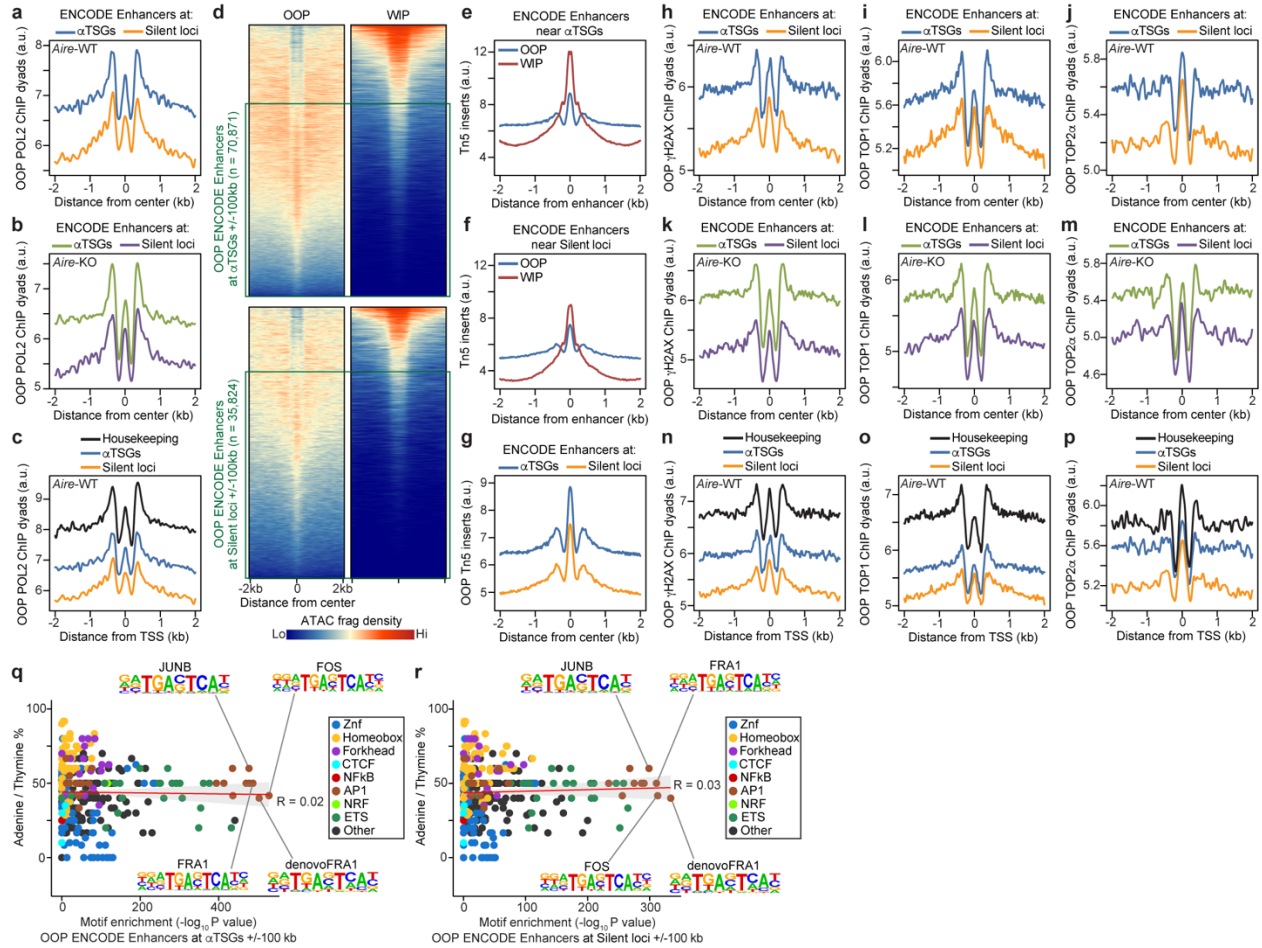
= 6,240: Immature=4,161, Transitional=858, Early Mature=667, Mid Mature=554). Box plots depict median, 25th and 75th percentile, whiskers represent 1.5 times interquartile range. P-values from one-sided Mann-Whitney U-tests. **h**, Aggregate ratios of normalized out-of-peak (OOP) or within-peak (WIP) scATAC-seq fragments from TSG^{pos} versus TSG^{neg} human mTECs at 1 Mb regions flanking tissue-specific genes. **i**, Distribution of out-of-peak (OOP) vs. within-peak (WIP) scATAC-seq fragment sizes from human mTECs. **j**, Aggregate prevalence of p53-target motifs across accessible mTEC genomes (*chromVAR* deviation scores) overlayed on scATAC-seq UMAP from (**a**). **k**, Transcription factor footprinting at p53-target motifs within each annotated scATAC-seq cluster from (**a**). **l**, Aggregate expression of p53-target genes overlayed on scATAC-seq UMAP from (**a**). **m**, Scatter plot comparing differential gene expression (scRNA-seq counts per million=CPM) of 51 known regulators of p53 activity between Early Mature and Immature mTECs versus Mid Mature and Immature mTECs. Benjamini-Hochberg FDR levels for the Mature vs. Immature mTEC comparison are indicated as point colors with highly significant differentially expressed genes (FDR $\leq 1e-9$, fold-change ≥ 2 or ≤ 0.5) indicated as repressors (brown text) or promoters (green text) of p53 activity. **n–u**, Expression levels of indicated genes overlayed on scATAC-seq UMAP from (**a**).



Supplementary Fig. 3: p53-hyperactivity is more deleterious than p53-deficiency to ectopic transcription in mTECs.

a,b, MA plots comparing differential expression of genes by bulk RNA-seq due to p53-deficiency (**a**) or p53-hyperactivity (**b**) in mature mTECs (n=3 biological replicates).

Densities of fold-change values are displayed on right margins. Statistically significant (Benjamini-Hochberg FDR ≤ 0.05) differential expression between the comparisons are highlighted in blue for all genes and red for AIRE-dependent tissue-specific genes (α TSGs).



Supplementary Fig. 4: Chromatin destabilization augments background accessibility at nearby enhancers.

a–c, Aggregate histograms of out-of-peak (OOP) ChIP-seq dyads over indicated loci in mature mTECs from indicated genotypes. **d**, Heatmaps of out-of-peak (left) or within-peak (right) scATAC-seq fragments from mature mTECs at known ENCODE distal enhancers within out-of-peak regions (highlighted in green) +/-100 kb of α TSGs (top) or Silent genes (bottom). **e,f**, Aggregate histogram of out-of-peak (blue) or within-peak (red) scATAC-seq inserts over known ENCODE distal enhancers within +/-100 kb of α TSGs (**e**) or Silent

genes (**f**) in mature mTECs. **g**, Aggregate histogram of out-of-peak (OOP) scATAC-seq inserts over known ENCODE distal enhancers within +/-100 kb of α TSGs (blue) or Silent genes (orange) in mature mTECs. **h–p**, Aggregate histograms of out-of-peak (OOP) ChIP-seq dyads over indicated loci in mature mTECs from indicated genotypes. **q,r**, Comparison of transcription factor motif enrichment within scATAC-seq fragments from mature mTECs mapping to out-of-peak (OOP) regions at indicated loci versus the adenine/thymine content of each motif. Trendlines (red) with 95% confidence intervals (gray) indicated.

Supplementary Discussion

We identified the tumor suppressor p53 as a key sensor of chromatin accessibility noise that potentially works to eliminate mTECs that ectopically activate genes specific to alternative lineages. To promote cellular plasticity for tolerance induction, we found that mTECs amplify chromatin accessibility noise through repression of p53 activity as part of its maturation program. The effect of this repression is consistent with p53's roles in maintaining lineage fidelity¹³, inhibiting somatic reprogramming¹⁴ and suppressing tumorigenesis¹⁵⁻¹⁷.

The robust expression of canonical p53 target genes and transcription factor footprinting at p53 target motifs we detected in immature mTECs from WT mice suggest that the p53-mediated 'quality-control' of chromatin stability is also active in the progenitor stages of normal mTEC development. Indeed, impairing the intrinsic apoptosis pathway in mTECs causes a selective increase in the numbers of only immature mTECs¹⁸, the sole developmental subset with substantial p53 activity. This p53-mediated selection of progenitors with stable chromatin may play an essential role in mTEC maturation as conditional deletion of *Trp53* in mTECs dampens responsiveness to NF- κ B signaling – the primary determinant of mTEC differentiation⁶⁻¹⁰ – and downstream processes associated with maturation⁵. These results suggest the dynamics of p53 activity across mTEC development counterbalance chromatin stability for maturation at early stages vs. chromatin instability for cellular plasticity at later stages.

For the mechanism driving the initial rise in chromatin accessibility noise, our results implicate an intrinsic role for the prevalence of nucleosome-destabilizing poly-AT tracts and other low complexity AT-rich motifs within the genomic regions flanking AIRE-dependent tissue-specific genes. This role is supported by the identification of a long poly-A tract (18-mer) as the most enriched motif within genomic regions that differ in sequence and chromatin accessibility – as well as the expression levels of the nearest α TSGs – between the maternal and paternal alleles of NOD x B6 F1 hybrid mice¹⁹. Considering

that chromatin destabilization can be first observed immediately following a hyperproliferative transit-amplifying stage in mTEC maturation, the hyperacetylated state of newly deposited histones²⁰ may make these AT-rich regions particularly susceptible to fluctuations in nucleosome dynamics. Consistent with the distal influence of poly-AT tracts on the nucleosome stability of its flanking regions^{12,21-23}, we found that the nearby tissue-specific enhancers have elevated baseline levels of chromatin accessibility and Pol II loading. These findings reinforce the role of chromatin state on stochastic gene expression, particularly the negative influence of nucleosome density on transcriptional initiation and burst frequency²⁴⁻²⁶.

In addition to the heightened background Pol II loading across genomic regions with chromatin accessibility noise, we also observed recruitment of topoisomerases and elevated levels of γ H2AX, which is the enzymatic product of the ATM kinase that phosphorylate p53 for activation²⁷. These results suggest that DNA damage serves as the connection between chromatin accessibility noise and p53-mediated cell death, consistent with previous reports associating elevated levels of γ H2AX and susceptibility to p53-dependent apoptosis²⁸. Elucidating the molecular mechanism that adjudicates the apoptotic response by p53 instead of DNA repair/survival in mTECs will be an important focus for future studies.

The mechanisms uncovered here in mTECs are potentially applicable to cellular plasticity observed in other contexts, such as tumorigenesis. Indeed, we found the chromatin destabilization at nucleosome-dense regions in lung adenocarcinomas to be associated with high plasticity states and regulated by p53. These results suggest a link between chromatin accessibility noise and phenotypic plasticity that facilitates the emergence of aggressive LUAD tumors^{16,17}. Despite sharing numerous traits commonly associated with tumorigenesis, thymic epithelial cancers are among the rarest malignancies²⁹. Investigating how mTECs avoid malignant transformation and how rare thymic epithelial cancers circumvent these checkpoints could reveal novel tumor-suppressive mechanisms.

Supplementary References

- 1 Huang, J. *et al.* p53 is regulated by the lysine demethylase LSD1. *Nature* **449**, 105-108 (2007). <https://doi.org:10.1038/nature06092>
- 2 Isbel, L. *et al.* Readout of histone methylation by Trim24 locally restricts chromatin opening by p53. *Nat Struct Mol Biol* **30**, 948-957 (2023). <https://doi.org:10.1038/s41594-023-01021-8>
- 3 Kim, J.-E., Chen, J. & Lou, Z. DBC1 is a negative regulator of SIRT1. *Nature* **451**, 583-586 (2008). <https://doi.org:10.1038/nature06500>
- 4 Zhao, W. *et al.* Negative regulation of the deacetylase SIRT1 by DBC1. *Nature* **451**, 587-590 (2008). <https://doi.org:10.1038/nature06515>
- 5 Rodrigues, P. M. *et al.* Thymic epithelial cells require p53 to support their long-term function in thymopoiesis in mice. *Blood* **130**, 478-488 (2017). <https://doi.org:10.1182/blood-2016-12-758961>
- 6 Burkly, L. *et al.* Expression of relB is required for the development of thymic medulla and dendritic cells. *Nature* **373**, 531-536 (1995). <https://doi.org:10.1038/373531a0>
- 7 Kajiura, F. *et al.* NF-kappa B-inducing kinase establishes self-tolerance in a thymic stroma-dependent manner. *J Immunol* **172**, 2067-2075 (2004). <https://doi.org:10.4049/jimmunol.172.4.2067>
- 8 Rossi, S. W. *et al.* RANK signals from CD4(+)3(-) inducer cells regulate development of Aire-expressing epithelial cells in the thymic medulla. *J Exp Med* **204**, 1267-1272 (2007). <https://doi.org:10.1084/jem.20062497>
- 9 Hikosaka, Y. *et al.* The cytokine RANKL produced by positively selected thymocytes fosters medullary thymic epithelial cells that express autoimmune regulator. *Immunity* **29**, 438-450 (2008). <https://doi.org:10.1016/j.immuni.2008.06.018>
- 10 Akiyama, T. *et al.* The tumor necrosis factor family receptors RANK and CD40 cooperatively establish the thymic medullary microenvironment and self-tolerance. *Immunity* **29**, 423-437 (2008). <https://doi.org:10.1016/j.immuni.2008.06.015>
- 11 Moore, J. E. *et al.* Expanded encyclopaedias of DNA elements in the human and mouse genomes. *Nature* **583**, 699-710 (2020). <https://doi.org:10.1038/s41586-020-2493-4>
- 12 Kornberg, R. D. & Stryer, L. Statistical distributions of nucleosomes: nonrandom locations by a stochastic mechanism. *Nucleic acids research* **16**, 6677-6690 (1988). <https://doi.org:10.1093/nar/16.14.6677>
- 13 Puisieux, A., Pommier, R. M., Morel, A.-P. & Lavial, F. Cellular Pliancy and the Multistep Process of Tumorigenesis. *Cancer cell* **33**, 164-172 (2018). <https://doi.org:https://doi.org/10.1016/j.ccell.2018.01.007>
- 14 Kawamura, T. *et al.* Linking the p53 tumour suppressor pathway to somatic cell reprogramming. *Nature* **460**, 1140-1144 (2009). <https://doi.org:10.1038/nature08311>

- 15 Kastenhuber, E. R. & Lowe, S. W. Putting p53 in Context. *Cell* **170**, 1062-1078 (2017).
[https://doi.org:https://doi.org/10.1016/j.cell.2017.08.028](https://doi.org/10.1016/j.cell.2017.08.028)
- 16 Marjanovic, N. D. *et al.* Emergence of a High-Plasticity Cell State during Lung Cancer Evolution. *Cancer cell* **38**, 229-246.e213 (2020).
[https://doi.org:10.1016/j.ccell.2020.06.012](https://doi.org/10.1016/j.ccell.2020.06.012)
- 17 Kaiser, A. M. *et al.* p53 governs an AT1 differentiation programme in lung cancer suppression. *Nature* **619**, 851-859 (2023). [https://doi.org:10.1038/s41586-023-06253-8](https://doi.org/10.1038/s41586-023-06253-8)
- 18 Jain, R. *et al.* How do thymic epithelial cells die? *Cell Death & Differentiation* **25**, 1002-1004 (2018). [https://doi.org:10.1038/s41418-018-0093-8](https://doi.org/10.1038/s41418-018-0093-8)
- 19 Fang, Y., Bansal, K., Mostafavi, S., Benoist, C. & Mathis, D. AIRE relies on Z-DNA to flag gene targets for thymic T cell tolerization. *Nature* **628**, 400-407 (2024).
[https://doi.org:10.1038/s41586-024-07169-7](https://doi.org/10.1038/s41586-024-07169-7)
- 20 Alabert, C. & Groth, A. Chromatin replication and epigenome maintenance. *Nature Reviews Molecular Cell Biology* **13**, 153-167 (2012). [https://doi.org:10.1038/nrm3288](https://doi.org/10.1038/nrm3288)
- 21 Segal, E. & Widom, J. Poly(dA:dT) tracts: major determinants of nucleosome organization. *Curr Opin Struct Biol* **19**, 65-71 (2009).
[https://doi.org:10.1016/j.sbi.2009.01.004](https://doi.org/10.1016/j.sbi.2009.01.004)
- 22 Ioshikhes, I. P., Albert, I., Zanton, S. J. & Pugh, B. F. Nucleosome positions predicted through comparative genomics. *Nat Genet* **38**, 1210-1215 (2006).
[https://doi.org:10.1038/ng1878](https://doi.org/10.1038/ng1878)
- 23 Segal, E. & Widom, J. From DNA sequence to transcriptional behaviour: a quantitative approach. *Nature reviews. Genetics* **10**, 443-456 (2009). [https://doi.org:10.1038/nrg2591](https://doi.org/10.1038/nrg2591)
- 24 Dey, S. S., Foley, J. E., Limsirichai, P., Schaffer, D. V. & Arkin, A. P. Orthogonal control of expression mean and variance by epigenetic features at different genomic loci. *Molecular Systems Biology* **11**, 806 (2015).
[https://doi.org:https://doi.org/10.15252/msb.20145704](https://doi.org/10.15252/msb.20145704)
- 25 Core, L. & Adelman, K. Promoter-proximal pausing of RNA polymerase II: a nexus of gene regulation. *Genes & development* **33**, 960-982 (2019).
[https://doi.org:10.1101/gad.325142.119](https://doi.org/10.1101/gad.325142.119)
- 26 Raj, A. & van Oudenaarden, A. Nature, nurture, or chance: stochastic gene expression and its consequences. *Cell* **135**, 216-226 (2008).
[https://doi.org:10.1016/j.cell.2008.09.050](https://doi.org/10.1016/j.cell.2008.09.050)
- 27 Fernandez-Capetillo, O., Lee, A., Nussenzweig, M. & Nussenzweig, A. H2AX: the histone guardian of the genome. *DNA Repair* **3**, 959-967 (2004).
[https://doi.org:https://doi.org/10.1016/j.dnarep.2004.03.024](https://doi.org/10.1016/j.dnarep.2004.03.024)
- 28 Dankert, J. F. *et al.* Cyclin F-Mediated Degradation of SLBP Limits H2A.X Accumulation and Apoptosis upon Genotoxic Stress in G2. *Mol Cell* **64**, 507-519 (2016).
[https://doi.org:10.1016/j.molcel.2016.09.010](https://doi.org/10.1016/j.molcel.2016.09.010)

- 29 Engels, E. A. Epidemiology of Thymoma and Associated Malignancies. *Journal of Thoracic Oncology* **5**, S260-S265 (2010).
[https://doi.org:https://doi.org/10.1097/JTO.0b013e3181f1f62d](https://doi.org/https://doi.org/10.1097/JTO.0b013e3181f1f62d)